Indonesian Journal of Aerospace Vol. 22 No. 2 Desember 2024 : pp 85 – 94 (Suraina et al.)
DOI: 10.59981/ijoa.2024.2942
https://ejournal.brin.go.id/ijoa/

Observations of Ionospheric Conditions Over Pontianak During The Partial Solar Eclipse

Suraina[1], Prayitno Abadi[2], Angga Yolanda Putra[3], Gerhana Puannandra Putri[1], Lambang Nurdiansah[4], Dadang Nurmali[1], Afif Rakhman[5], Ednofri[6] and Muzirwan[2]

[1]Research Center for Space, National Research and Innovation Agency, Indonesia
[2]Research Center for Climate and Atmosphere, National Research and Innovation Agency, Indonesia
[3]Pontianak Observatory for Space and Atmosphere, National Research and Innovation Agency, Indonesia
[4]Center for Data and Information, National Research and Innovation Agency, Indonesia
[5]Mathematics and Natural Sciences, Gadjah Mada University of Seventh Author , Indonesia
[6]Agam Observatory for Space and Atmosphere, National Research and Innovation Agency, Indonesia
e-mail: [1]sura019@brin.go.id

Received: 18-12-2023. Accepted: 19-06-2024. Published: 20-05-2025

Abstract

Solar energy plays a significant role in creating ionospheric layers through photoionization. However, when a solar eclipse occurs, the ionizing radiation from the sun will be obstructed by the moon, resulting in a decrease in ionization processes and a depletion of ionospheric plasma density. Our research examines the effects of two partial solar eclipse events that occurred on December 26, 2019 (Eclipse 1) and April 20, 2023 (Eclipse 2) over Pontianak. We observed changes in f_oF_2 and TEC during these events. Our observations show that f_oF_2 and TEC decreased at the start of a partial eclipse but returned to normal once the eclipse ended. The maximum decrease in f_oF_2 observed was 1.88 MHz for Eclipse 1 and 1.26 MHz for Eclipse 2, while the decreases in TEC were 5.68 and 12.81 TECU for Eclipse 1 and 2 respectively. We noted that geomagnetic activity was quiet during both eclipses, indicating that the reduction in ionospheric parameters (TEC and f_oF_2) is affected by the solar eclipse. During a solar eclipse, the decrease in ionization intensity results in a reduction in electron numbers in the ionospheric layers, leading to a reduction in TEC and f_oF_2.

Keywords**:** *Partial solar eclipse, Critical frequency, Total electron content, Declining phase, Recovery phase.*

1. Introduction

The Sun is the primary source of energy in the solar system. The Sun is constantly emanating electromagnetic radiation and high energy particles, with Sun or solar activities such as sunspots, solar wind, solar flares, and CMEs affecting the intensity of the radiation. The solar radiation and particles then interact with the interplanetary medium, the planet's magnetosphere, and even the planet's atmosphere. The fluctuation and dynamic nature of the space environment caused by solar activities is called space weather, especially around the Earth.

Space weather studies the effect of solar activities and radiation on the space environment around the Earth, including the magnetosphere, ionosphere, and thermosphere. The dynamic in those environments could cause disturbance in many technological aspects, such as satellites, communication, and navigation signals, and in some extreme cases, the electrical grid on the Earth's surface. With so many life aspects now heavily dependent on technology, it become important to understand the dynamics and effects of space weather and develop safety measures to mitigate the impact on life on Earth.

The ionosphere is one of the Earth's atmospheric layers and plays an important part in communication and navigation technology. The ionosphere layer has an altitude of 60

km to 1000 km. The ionosphere layer acts as a medium for propagating radio waves. The ionospheric layer is formed by solar radiation, including X-rays and EUV. The radiation converts neutral molecules in the ionospheric layer into charged particles that are dynamic. A large influx of X-rays and EUV from the Sun can increase the ionization, dissociation, and heating in the ionosphere, causing disturbances in the electron and plasma temperature, density, and dynamics (Maodong Yan et. al, 2022). This dynamic nature of the ionosphere layer can affect the performance of space-based technologies, which in turn impact life on Earth. To obtain information about the characteristics of ionospheric changes, continuous ionospheric observations are needed. These observations monitor changes in ions and electrons, which indicate space weather changes. Some ionospheric parameters that can indicate changes in the ionospheric layer include Total Electron Content (TEC) and critical frequency of the F_2 layer (f_oF_2). These parameters are highly dependent on solar radiation intensity.

A solar eclipse is a phenomenon that occurs when the Moon is between the Sun and the Earth. Solar energy plays a significant role in creating ionospheric layers through photoionization, so its variations depend on solar activity. During a solar eclipse, the Moon's shadow in the eclipse region covers the ionospheric layer, temporarily halting the solar radiation that ionizes the ionospheric layer. At that time, the photoionization process decreases (Rishbeth, 1970), ultimately reducing ionospheric conductivity and affecting the values of ionospheric layer parameters.

In the case of the solar eclipse on January 26, 2009, there was a decrease in f_oF_2 values over Kototabang, Pontianak, and Pameungpeuk, with a maximum decrease of ~0.5 MHz, ~2 MHz, and ~0.5 MHz respectively (Perwitasari & Muslim, 2009). Ionosonde data in Australia and Antarctica (middle and high latitudes) showed a decrease in f_oF_2 during the solar eclipse on April 29, 2014 (R. Atulkar, et al., 2015). The value of f_oF_2 also decreased by 4 MHz over Biak during the solar eclipse on March 9, 2016 (Dear et al., 2020), and the Total Electron Content (TEC) experienced a decrease of approximately 12 TECU based on GPS data from Palu (Muslim et al., 2016). Research on the ionospheric response to solar eclipses has been conducted, but it has not covered the entire Earth's surface. Considering that solar eclipses are localized events and the ionospheric characteristics are regional, it is necessary to conduct more research on them.

This study intends to investigate the ionospheric response to a partial solar eclipse over Pontianak, namely the Annular Solar Eclipse of 2019 and the Hybrid Solar Eclipse of 2023. The ionosphere's response to a solar eclipse can be related to reduced ionization, resulting in the expected depletion of ionospheric plasma density. It will gradually recover as the Moon moves away from the sun-earth line. At that time, the photosphere of the sun slowly started to emit high radiation, and it is expected that there will be an increase in X-rays, resulting in an increase in ionization during the eclipse stage. This depletion is also influenced by the extent of solar radiation obscured by the moon.

2. Methodology

The data used in this study are Total Electron Content (TEC) and critical frequency of the F_2 layer (f_oF_2) from the Pontianak Station equipment (0.03°LS, 109.33°E longitude). The solar eclipse event data used in this paper are the Annular Solar Eclipse on December 26, 2019 (eclipse 1) and the Hybrid Solar Eclipse on April 20, 2023 (eclipse 2). Eclipse 1 lasts from 03:45 UT to 07:32 UT, with the maximum eclipse occurring at 05:44 UT with an obscuration of 93.24%. Meanwhile, eclipse 2 lasts from 02:49 UT to 05:20 UT, with the maximum eclipse occurring at 04:03 UT with an obscuration of 30.98%.

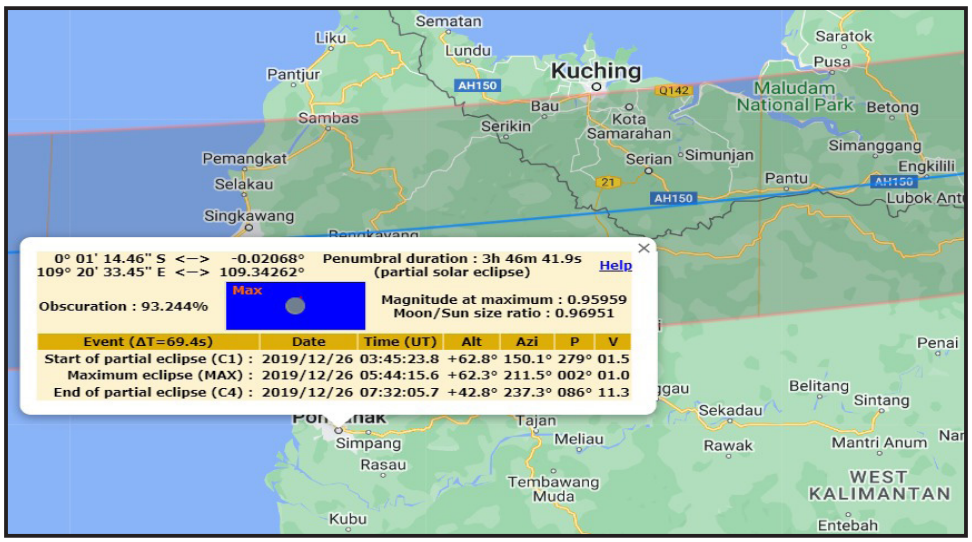

Figure 2-1: The path of the annular solar eclipse on December 26, 2019 with the eclipse's parameter for Pontianak (https://eclipse.gsfc.nasa.gov/SEpath).

Figure 2-2: The path of the annular solar eclipse (blue and pink line) on April 20, 2023 with the eclipse's parameter for Pontianak (https://eclipse.gsfc.nasa.gov/SEpath).

In eclipse 2, we also use foF2 data from the Darwin Station (12.45°LS, 130.85°E longitude), where the eclipse lasts from 02:47 UT to 05:55 UT, with the maximum eclipse occurring at 04:22 UT with an obscuration of 80.66%.

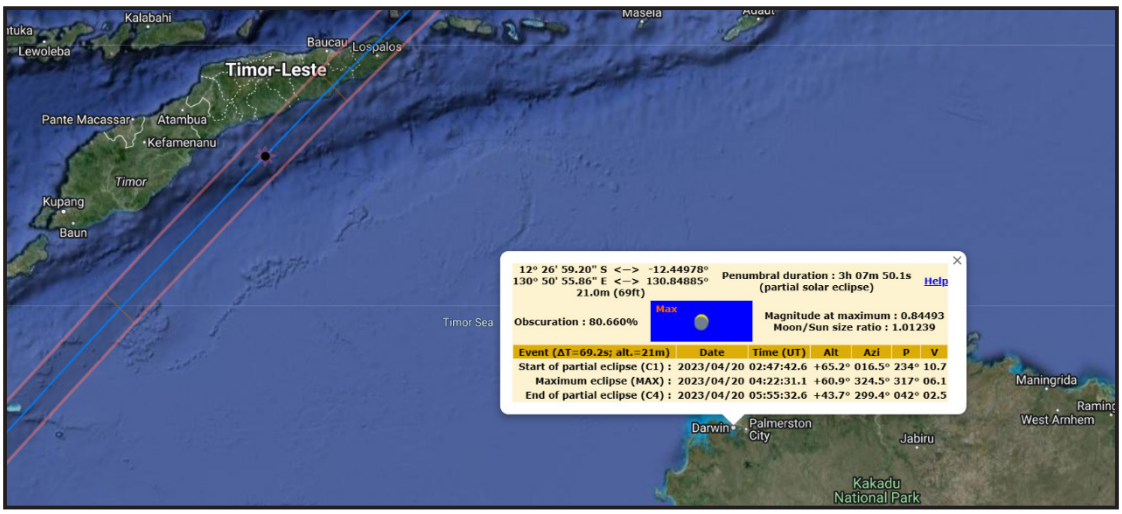

Figure 2-3: The path of the annular solar eclipse (blue and pink line) on April 20, 2023 with the eclipse's parameter for Darwin (https://eclipse.gsfc.nasa.gov/SEpath).

TEC data was obtained from recordings of GISTM (GPS Ionospheric TEC and Scintillation Monitor) in 2019 and Septentrio in 2023. The GISTM used has a sampling resolution of 50Hz. TEC is stated in TEC Units (TECU), where one TECU equals 10^6 10^6 electrons per square meter (10^6 10^6 el/m^2m^2). The TEC ionosphere can be estimated using dual-frequency GPS, but these estimates still contain instrumental biases consisting of receiver Differential Code Bias (DCB) (Choi, 2010) and satellite DCB. To ensure that the observed TEC values approximate the true TEC values, instrumental biases need to be estimated during vertical Total Electron Content (VTEC) computation.

Assuming that Slant TEC (STEC), or TEC along the path of the GPS signal from the satellite to the GPS receiver, has the same influence on GPS signal propagation along the thin ionospheric layer at an altitude of 350 km from the Earth's surface, the STEC value derived from GPS data can be converted to VTEC using an equation (Muslim, 2011).

$$STEC = M(z)\ x\ VTEC + b_p + B_pSTEC = M(z)\ x\ VTEC + b_p + B_p \quad (2\text{-}1)$$

Where M(z) is a mapping function expressed as.

$$M(z) = \left[1 - \left(\frac{R_e}{R_e + H}\right)^2 sin^2 z\right]^{1/2} \quad (2\text{-}2)$$

With z as the zenith angle of the GPS satellite, Re as the radius of the Earth, and H as the height of the ionospheric layer (assumed to be 350 km), bp and Bp are the respective biases of the satellite and receiver DCB. Olla et al. (2022) asserts, "Vertical TEC can be calculated using the equation provided by Rothacher and Mervart"

$$VTEC = STEC\left[1 - \left(\frac{R_e}{R_e + H}\right)^2 cos^2 E\right]^{1/2} \quad (2\text{-}3)$$

with E as the inclination angle formed between the satellite and the receiving station (°).

f_oF_2 data is obtained from the observations of ionosonde, specifically the Canadian Advanced Digital Ionosonde (CADI). The Ionosonde emits radio wave signals in the frequency range of 1.6–24 MHz. Signal transmission is repeated every 15 minutes. The received signals from the ionospheric layer are recorded as an ionogram. The ionogram is scaled every 5 minutes during a solar eclipse to obtain f_oF_2.

To determine the changes that occur in TEC, f_oF_2, and the geomagnetic Sq field during a solar eclipse, each of these parameters is compared with reference values. VTEC was compared to the average variation of VTEC on five quiet geomagnetic days, and f_oF_2 was compared to its monthly median value. The selection of five quiet days is based on international regulations that determine the five most quiet days in the eclipse month.

The quiet geomagnetic day pattern has been established by international rules, divided into two parts within a month: a total of 10 days most disturbed and 5 days most quiet. Those

rules are used by world experts as the basis for analyzing the daily variations of the H-component in the quiet day pattern. The empirical model of daily variation of H-component quiet days (Mamat., 2006) is determined based on the average daily variation of the H-component over five quiet days using Harmonic analysis method. Information on the five international quiet days is obtained from the World Data Center (WDC). The reference value we use to analyze VTEC changes is obtained by calculating the Mean of the five quietest days' VTEC Sq (H) within one month. The VTEC data of the five quietest days are averaged at the same minute to obtain a daily VTEC value in minute intervals, which is used as the reference day.

3. Result and Analysis

During a Solar Eclipse, the moon fully or partially blocks the sun. This results in the intensity of solar radiation reaching the Earth's atmosphere or ionosphere layer being reduced. As a consequence, there is a reduced ionization in the ionospheric layer, where the photoionization process produces ions and electrons. The electron concentration in the ionosphere can be expressed by the TEC value.

The response of TEC to the solar eclipse event on December 26, 2019, has been reported by Aa et al. (2020) based on observations in the Indian equatorial latitudes and Asian longitude sectors. Their analysis results indicated a depletion of TEC by up to 6 TECu (50%) above equatorial stations. Similar depletion was also found in our study results. The results of TEC data analysis during the solar eclipse on December 26, 2019, and April 20, 2023, over Pontianak are shown in Figure 3-1. In the figure, the black curve represents the average VTEC during the five days of quiet geomagnetic activity. In comparison, the blue curve represents daily VTEC data. It appears that on the eclipse day, December 26, 2019, a decrease in VTEC values relative to the average VTEC was observed from 04:35 UT to 09:38 UT. This period coincides with the time range of the eclipse event. The decrease in VTEC began at 04:35 UT with a value of 22 TECU, or approximately 50 minutes after the partial solar eclipse began. The decrease in VTEC continues alongside the level of eclipse obscuration reduces. The maximum VTEC decrease occurs around 06:09 UT, with a decrease of 5.68 TECU (23%) relative to the average VTEC simultaneously. The maximum decrease occurs approximately 25 minutes after the peak of the solar eclipse. After that, the VTEC value experienced a recovery where it gradually increased until 09:38 UT, along with the increase in the level of eclipse shadow with a VTEC value of 23 TECU.

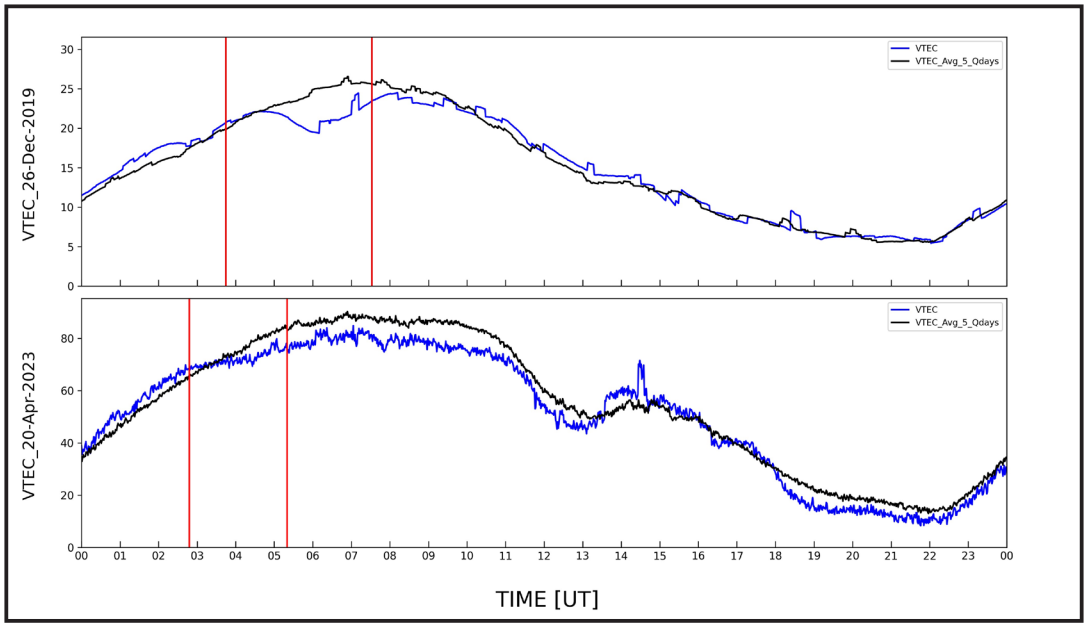

Figure 3-1: VTEC values (blue line) relative to the average variation of VTEC (black line) on December 26, 2019 (top) and April 20, 2023 (bottom).

VTEC values also decreased during the Partial Solar Eclipse on April 20, 2023, shown in Figure 3. It is observed that the decrease in VTEC begins at 03:35 UT with a VTEC value = 71 TECU, or approximately 47 minutes after the partial solar eclipse began. The decrease of

VTEC is relatively smooth, with the maximum decrease occurring around 07:51 UT at 12.81 TECU (15%) relative to the average VTEC simultaneously. The VTEC recovery phase lasted until 13:24 UT with a VTEC value of 52 TECU.

From both observation results, it can be inferred that the decrease in TEC during eclipse 1 (23%) is greater than the decrease in TEC during eclipse 2 (15%). However, the duration of TEC decrease during Eclipse 2 is longer than Eclipse 1. The decrease in TEC during eclipse 1 lasted approximately 5 hours and 3 minutes, while the decrease in TEC during eclipse 2 lasted about 9 hours and 49 minutes. In addition, from Figure 3, we can observe different characteristics of the TEC curve decreasing. For Eclipse 1, the decrease in TEC occurs drastically in a relatively short time. Meanwhile, for Eclipse 2, the decrease in TEC occurs monotonically but remains below average values. When a solar eclipse occurs in the morning, the Total Electron Content (TEC) has a longer recovery period (Chen et al, 2023). According to them, one contributing factor to this behavior is that geomagnetic conditions in the morning are not so quiet. Similar observations have been reported by Deshpande et al. (1977) regarding the Equatorial Electrojet (EEJ) effects on TEC over the Indian sector. They speculate that the electron density returns to reference values after several hours due to the delaying factor of recombination during a solar eclipse.

Observations of f_oF_2 during the solar eclipse on December 26, 2019, and April 20, 2023, are shown in Figure 3-2. In the figure 3-2, the black curve represents the monthly median of f_oF_2. While the blue curve represents daily f_oF_2 data. It appears that on the eclipse day, December 26, 2019, and April 20, 2023, a decrease was observed. It seems that the f_oF_2 value in the case of eclipse 1 begins to decrease after 02:45 UT or about 60 minutes before the eclipse begins, with a f_oF_2 value of 6.47 MHz. The f_oF_2 value continued to decrease as the level of eclipse shadow decreased, reaching the lowest value of f_oF_2 = 4.97 MHz at 07.30 UT or approximately 106 minutes after the eclipse peak (at 05.44 UT). The f_oF_2 value at this time decreased by 1.88 MHz (27%) relative to the monthly median value. After that, the f_oF_2 value recovered, where it increased again as the eclipse shadow increased until 09.00 UT with a f_oF_2 value of 6.86 MHz.

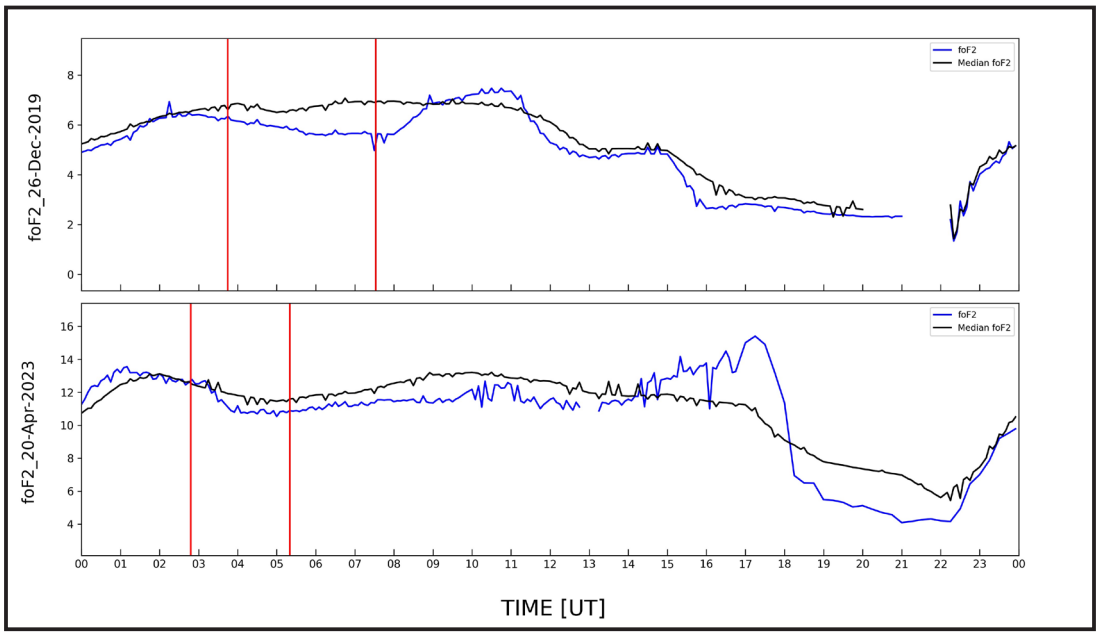

Figure 3-2: f_oF_2 values (blue line) relative to monthly median of f_oF_2 (black line) on December 26, 2019 (top) and April 20, 2023 (bottom).

From Figure 3-2, observe that the f_oF_2 value began to decrease after 01:15 UT or approximately 93 minutes before the first contact of the solar eclipse, with a f_oF_2 value of 13.4 MHz. As the level of eclipse shadow decreases, the f_oF_2 value decreases until it reaches its lowest value, foF2 = 10.69 MHz at 04:00 UT or about 3 minutes before the eclipse peak time. The maximum decrease of f_oF_2 during this eclipse event is 1.26 MHz (10%) relative to the monthly

median value. The f_oF_2 value continued to fluctuate and lasted until 14:15 UT, with f_oF_2 values still below its median value. The duration of the f_oF_2 decrease from eclipse 2 to the recovery phase is approximately 13 hours. This duration is longer than the duration of the f_oF_2 decrease during Eclipse 1, which only lasts about 6 hours and 15 minutes.

In eclipse 2, the changes in TEC and f_oF_2 are not significant based on observations at the Pontianak station. Possibly because the eclipse path was far from Pontianak, resulting in relatively small obscuration at that time. Therefore, as a comparison, we used data from the Darwin station, which is closer to the eclipse path. However, we can only display f_oF_2 data, due to limitations in obtaining TEC data at that location. The change in f_oF_2 values during the solar eclipse on April 20, 2023, based on observations from the Darwin station, is presented in Figure 3-3.

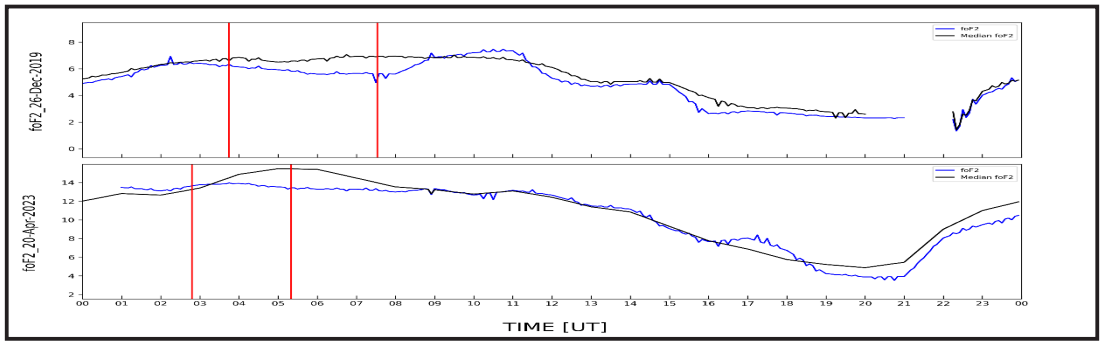

Figure 3-3: f_oF_2 values (blue line) relative to monthly median of f_oF_2 (black line) on April 20, 2023 based on observations from the Darwin station.

From Figure 3-3, observe that the f_oF_2 value began to decrease after 03:30 UT or about 30 minutes after the first contact of the solar eclipse, with a f_oF_2 value of 13.84 MHz. The decrease in f_oF_2 values was relatively constant, lasting for approximately 5 hours and 15 minutes. The maximum decrease of f_oF_2 occurred at 05:15 UT or about 53 minutes after the maximum eclipse phase, with a maximum decrease of approximately 14.11% (2.18 MHz). After 08:45 UT, the f_oF_2 value recovered, where it increased again as the eclipse shadow increased with a f_oF_2 value of 13.35 MHz.

Table 3-1: Parameter comparison between the December 26th, 2019 and April 20th, 2023 eclipses

Parameter	December 26th, 2019	April 20th, 2023 (Pontianak)	April 20th, 2023 (Darwin)
First eclipse contact	03.45 UT	02.48 UT	02.47 UT
Maximum	05.44 UT	04.03 UT	04.22 UT
Last eclipse contact	07.32 UT	05.20 UT	05.55 UT
Obscuration	93.244 %	31.040 %	80.66 %
f_oF_2 -TEC decreases time difference	1 hr 50 min	2 hr 20 min	-
f_oF_2 -TEC recovery time difference	38 min (before TEC)	51 min (after TEC)	-
VTEC relative decrease	23 %	15%	-
f_oF_2 relative decrease	27%	10%	14%

Electron density has a positive correlation with f_oF_2 values, a decrease in TEC is accompanied by a decrease in f_oF_2. Similar to TEC, the decrease in f_oF_2 during eclipse 1 (27%) is also larger than the decrease in f_oF_2 during eclipse 2 (10%). This could be due to the differences in obscuration within an eclipse zone. Obscuration can reduce solar radiation above the zone traversed by the eclipse (Bravo et al., 2020; Cherniak & Zakharenkova, 2018; Coster et al., 2017; Eisenbeis & Occhipinti, 2021; Shrivastava et al., 2021). In the case of Eclipse 1 with an obscuration value of 93%, it has a greater impact compared to Eclipse 2 with an obscuration level of 31%. The larger the obscuration, the lower the intensity of sunlight reaching the ionospheric layer. Chen et al. (2023) believe that the maximum obscuration of 16.6% at Jicamarca in the total solar eclipse causes significant attenuation of EUV solar irradiance, thereby impeding the equatorial electrodynamics processes.

Table 3-2: Result comparison for TEC and foF2 decrease for several eclipses and locations

Parameter	Obscuration	TEC decrease	f_oF_2 decrease
December 26th, 2019: Pontianak (this paper)	93.244%	23%	27%
April 20th, 2023: Pontianak (this paper)	31.040%	15%	10%
April 20th, 2023: Darwin (this paper)	80.66%	-	14%
March 9th, 2016: Biak (Dear et.al., 2020)	87.29%	33%	~40%
March 9th, 2016: Guam (Dear et.al., 2020)	82.88%	22%	30%

In eclipse 1, the f_oF_2 value begins to decrease 1 hour 50 minutes before the TEC value decreases. Similarly, the recovery time of f_oF_2 is 38 minutes faster before the TEC value starts to recover. In the case of eclipse 2, the f_oF_2 descent time is 2 hours and 20 minutes faster before the TEC value decreases. However, the recovery time of f_oF_2 is 51 minutes slower after the TEC value recovers. The recovery time of TEC and f_oF_2 values in eclipse 2 does not immediately occur several minutes after the eclipse ends, and the decrease in values also lasts longer. Even though the solar eclipse has ended, the values of TEC and f_oF_2 continue to experience a prolonged decrease.

4. Conclusions

The partial solar eclipse effect on the ionosphere over Pontianak was analyzed using TEC (Total Electron Content) and f_oF_2 (critical frequency of the F_2 layer), namely the Annular Solar Eclipse on December 26, 2019, and the Hybrid Solar Eclipse on April 20, 2023. During both eclipses, geomagnetic activity was quiet. We observed that the ionospheric plasma density changes as the solar eclipse passes. TEC and f_oF_2 data show the impact of the Solar Eclipse on December 26, 2019, resulting in a decrease in VTEC relative to the average VTEC of 23% and a decrease in f_oF_2 relative to the monthly median of 27%. Meanwhile, for the Solar Eclipse on April 20, 2023, there was a decrease in TEC and f_oF_2 data by 15% and 10%, respectively. Based on observations from the Darwin station on April 20, 2023, f_oF_2 also experienced a decrease of 14% relative to the monthly median value. From the results, we can conclude that both eclipses with different characteristics have different impacts. The impact depends on the obscuration of the eclipse and its path.

Acknowledgements

This study was financially supported by the Research Organization for Aeronautics and Space, National Research and Innovation Agency (BRIN). The author would like thank to NASA's official website at NASA Homepage, https://eclipse.gsfc.nasa.gov/SEpath for solar eclipse data used in this study and SOAA Pontianak for GISTM/Septentrio-CADI-Magnetometer data. The author would also like to thank La Ode Muhammad Musafar Kilowasid (Directorate of Laboratory Management, Research Facilities, and Science and Technology Park – Coordinator) who helped evaluate the manuscript. The author would also like to thank the anonymous reviewers of IJOA (Indonesian Journal of Aerospace) for valuable comments that improved the quality of this paper.

Contributorship Statement

Contributorship in this article is as follows, Su, PA, FA, AYP, GPP, LN, AR, Ed, Mu, and DN. Su designed the method, preprocessed CADI data, analyzed the results, and prepared the manuscript; PA analyzed the results; AYP developed the simulation, preprocessing GISTM and Magnetometer data; GPP prepared the manuscript; LN preprocessed CADI data; DN preprocessed CADI data; AR help evaluate the manuscript; Ed carried out the availability of

GISTM data; Mu carried out the availability of Magnetometer data.

References

Aa, E., Zhang, S. R., Erickson, P. J., Goncharenko, L. P., Coster, A. J., Jonah, O. F., et al. (2020). Coordinated ground-based and space-borne observations of ionospheric response to the annular solar eclipse on 26 December 2019. *Journal of Geophysical Research: Space Physics*, 125, e2020JA028296. https://doi.org/10.1029/2020JA028296

Atulkar, R., Khan, P. A., Jeevakhan, H., & Purohit, P. K. (2015). Ionospheric response to annular and partial solar eclipse of 29 April 2014, in Antarctica and Australian Regions. *Russian Journal of Earth Sciences*, 15(2), 1-8. https://doi.org/10.2205/2015ES000549

Bravo, M., Martínez-Ledesma, M., Foppiano, A., Urra, B., Ovalle, E., Villalobos, C., et al. (2020). First report of an eclipse from Chilean ionosonde observations: Comparison with total electron content estimations and the modeled maximum electron concentration and its height. *Journal of Geophysical Research: Space Physics*, 125, e2020JA027923. https://doi.org/10.1029/2020JA027923

Chen, S. S., Resende, L. C. A., Denardini, C. M., Chagas, R. A. J., Da Silva, L. A., Marchezi, J. P., et al. (2023). The 14 December 2020 Total Solar Eclipse effects on geomagnetic field variations and plasma density over South America. *Journal of Geophysical Research: Space Physics*, 128, e2022JA030775. https://doi.org/10.1029/2022JA030775

Cherniak, I., & Zakharenkova, I. (2018). Ionospheric total electron content response to the great American solar eclipse of 21 August 2017. *Geophysical Research Letters*, 45, 1199–1208. https://doi.org/10.1002/2017GL075989

Choi, B.K., Chung, J.K., & Cho, J.H. (2010). Receiver DCB Estimastion and Analysis by Type of GPS Receiver, J. Astron. *Space Sci.*, 27(2), 123-128. https://doi.org/10.5140/JASS.2010.27.2.123

Coster, A. J., Goncharenko, L., Zhang, S.-R., Erickson, P. J., Rideout, W., & Vierinen, J. (2017). GNSS observations of ionospheric variations during the 21 August 2017 solar eclipse. *Geophysical Research Letters*, 44, 12041–12048. https://doi.org/10.1002/2017GL075774

Dear, V., Husin, A., Anggarani, S., Harjosuwito, J., & Pradipta, R. (2020). Ionospheric effects during the total solar eclipse over Southeast Asia-Pacific on 9 March 2016: Part 1. Vertical movement of plasma layer and reduction in electron plasma density. *Journal of Geophysical Research: Space Physics*, 125(5), 1-15. https://doi.org/10.1029/2019JA026708

Deshpande, M. R., Rastogi, R. G., Vats, H. O., Klobuchar, J. A., Sethia, G., Jain, A. R., et al. (1977). Effect of electrojet on the total electron content of the ionosphere over the Indian subcontinent. *Nature*, 267(5612), 599–600. https://doi.org/10.1038/267599a0

Eisenbeis, J., & Occhipinti, G. (2021). TEC depletion generated by the total solar eclipse of 2 july 2019. *Journal of Geophysical Research: Space Physics*, 126, e2021JA029186. https://doi.org/10.1029/2021JA029186

Mamat. R., Sity R., Habirun, & Visca. W. (2010) Penentuan pola hari tenang untuk mendapatkan tingkat gangguan geomagnet di Biak, *Majalah Sains Teknologi Dirgantara*, 1(2), 103 – 113. https://jurnal.lapan.go.id/index.php/majalah_sains_tekgan/article/download/421/361

Maodong Yan, Tong Dang, Yu-Tian Cao, Jun Cui, Binzheng Zhang, Zerui Liu, & Jiuhou Lei. (2022). A Comparative Study of Ionospheric Response to Solar Flares at Earth, Venus, and Mars. *The Astrophysical Journal*, 939, 23. https://doi.org/10.3847/1538-4357/

ac92ff

Muslim, B. (2011). Estimasi TEC dan Bias Instrumental Untuk Penguatan Navigasi GPS. *Prosiding Siptekgan*. 497-500. https://karya.brin.go.id/id/eprint/10622

Muslim, B., Sunardi, B., Merdijanto, U., Heryanto, D.T., Efendi, J., & Andrian, Y. (2018). Analisisi Respon Ionosfer Terhadap Gerhana Matahari 9 Maret 2016 dari Data GPS Palu. *Jurnal Meteorologi dan Geofisika*, 17(3). https://doi.org/10.31172/jmg.v17i3.328

Olla, A., Husin, A., Warsito, A., & Boimau, Y. (2022). Analisis Variasi Jumlah Kandungan Elektron Ionosfer Daerah Kupang (10,9°LS – 123°BT). *Journal for Physics Education and Applied Physics*, 4(1). DOI : 10.37058/diffraction.v4i1.5284

Perwitasari, S. & Muslim, B.: Respon ionosfer terhadap gerhana Matahari 26 Januari 2009 dari pengamatan ionosonda. *In: Seminar Nasional Penelitian, Pendidikan, dan Penerapan MIPA*, pp. 501-506. Universitas Negeri Yogyakarta (2009). http://eprints.uny.ac.id/id/eprint/12313

Rishbeth, H. (1970). Eclipse effects in the ionosphere. *Nature*, 226(5251), 1099–1100. https://doi.org/10.1038/2261099a0

Shrivastava, M. N., Maurya, A. K., & Kumar, K. N. (2021). Ionospheric perturbation during the South American total solar eclipse on 14th December 2020 revealed with the Chilean GPS eyeball. *Scientific Reports*, 11(1), 1–13. https://doi.org/10.1038/s41598-021-98727-w